JVI Journals.ASM.org

The M Segment of the 2009 Pandemic Influenza Virus Confers Increased Neuraminidase Activity, Filamentous Morphology, and Efficient Contact Transmissibility to A/Puerto Rico/8/1934-Based Reassortant Viruses

Patricia J. Campbell,[b] Shamika Danzy,[a] Constantinos S. Kyriakis,[a] Martin J. Deymier,[c] Anice C. Lowen,[a] John Steel[a]

Department of Microbiology and Immunology, Emory University School of Medicine, Atlanta, Georgia, USA[a]; Microbiology and Molecular Genetics Graduate Program[b] and Emory Vaccine Center at Yerkes National Primate Research Center,[c] Emory University, Atlanta, Georgia, USA

ABSTRACT

The 2009 H1N1 lineage represented the first detection of a novel, highly transmissible influenza A virus genotype: six gene segments originated from the North American triple-reassortant swine lineage, and two segments, NA and M, derived from the Eurasian avian-like swine lineage. As neither parental lineage transmits efficiently between humans, the adaptations and mechanisms underlying the pandemic spread of the swine-origin 2009 strain are not clear. To help identify determinants of transmission, we used reverse genetics to introduce gene segments of an early pandemic isolate, A/Netherlands/602/2009 [H1N1] (NL602), into the background of A/Puerto Rico/8/1934 [H1N1] (PR8) and evaluated the resultant viruses in a guinea pig transmission model. Whereas the NL602 virus spread efficiently, the PR8 virus did not transmit. Swapping of the HA, NA, and M segments of NL602 into the PR8 background yielded a virus with indistinguishable contact transmissibility to the wild-type pandemic strain. Consistent with earlier reports, the pandemic M segment alone accounted for much of the improvement in transmission. To aid in understanding how the M segment might affect transmission, we evaluated neuraminidase activity and virion morphology of reassortant viruses. Transmission was found to correlate with higher neuraminidase activity and a more filamentous morphology. Importantly, we found that introduction of the pandemic M segment alone resulted in an increase in the neuraminidase activity of two pairs of otherwise isogenic PR8-based viruses. Thus, our data demonstrate the surprising result that functions encoded by the influenza A virus M segment impact neuraminidase activity and, perhaps through this mechanism, have a potent effect on transmissibility.

IMPORTANCE

Our work uncovers a previously unappreciated mechanism through which the influenza A virus M segment can alter the receptor-destroying activity of an influenza virus. Concomitant with changes to neuraminidase activity, the M segment impacts the morphology of the influenza A virion and transmissibility of the virus in the guinea pig model. We suggest that changes in NA activity underlie the ability of the influenza M segment to influence virus transmissibility. Furthermore, we show that coadapted M, NA, and HA segments are required to provide optimal transmissibility to an influenza virus. The M-NA functional interaction we describe appears to underlie the prominent role of the 2009 pandemic M segment in supporting efficient transmission and may be a highly important means by which influenza A viruses restore HA/NA balance following reassortment or transfer to new host environments.

The 2009 influenza pandemic was caused by an H1N1 subtype influenza A virus that originated in the swine reservoir. Although swine influenza viruses, including H1N1 subtype strains, are occasionally detected in humans who have had direct contact with pigs, these are most often isolated events which do not lead to sustained human-to-human spread (1–6). Clearly, the 2009 pandemic H1N1 influenza A viruses transmit with significantly greater efficiency among humans than do swine influenza isolates. Given that all eight gene segments of the pandemic strain derive from influenza A viruses that have been circulating in swine for at least 10 years, this raises the important question of what viral factors permit efficient human-to-human transmission. One novel feature of the 2009 pandemic virus which appears to play a role is the presence of two gene segments from the avian-like Eurasian swine lineage in the context of a North American triple reassortant swine virus background (7–12).

Efforts over recent several years to identify the viral factors required for spread of influenza A virus between mammals have revealed that transmissibility is a complex, multigenic trait. The receptor binding specificity (13, 14) and the acid stability (15, 16) of the hemagglutinin (HA) glycoprotein appear to be important factors, and the viral polymerase complex has been seen to contribute to the transmission phenotype (17, 18). Nevertheless, it has also been shown that neither an HA protein which binds human type receptors nor viral replication machinery (as encoded by the 6 internal genes) adapted to growth in human cells is sufficient to

Received 5 December 2013 **Accepted** 12 January 2014
Published ahead of print 15 January 2014
Editor: D. S. Lyles
Address correspondence to John Steel, john.steel@emory.edu.

doi:10.1128/JVI.03607-13

support transmission of influenza viruses between ferrets (19). To date, the set of viral traits sufficient to give rise to a fully transmissible phenotype in humans has yet to be identified. Previous studies on the 2009 pandemic strain suggest that determinants residing in the M segment (9, 11, 12), which encodes the matrix (M1) and proton channel (M2) proteins, as well as the NA gene (10–12), which encodes the neuraminidase (NA) protein, contribute to transmissibility.

The matrix protein forms a structural layer under the viral envelope through interaction with the viral glycoproteins HA and NA (20, 21) and is thought to subsequently recruit the viral ribonucleoprotein (vRNP) complexes during assembly (20–22). M2 is a transmembrane channel protein that is involved in (i) membrane scission during viral egress (23); (ii) acidification of the virion during viral entry, which leads to release of vRNPs from the M1 protein (24–27); and (iii) preventing premature conformational change of specific hemagglutinin proteins in the Golgi complex, mediated through control of the pH within this organelle (24, 25, 27). Both M1 and M2 have been identified as determinants of influenza virion morphology (28–33), and point mutations in either protein can convert an exclusively spherical influenza virus (approximately 200 nm diameter) to one that produces a mixture of spheres and filaments (which can be greater than 1 μm in length) and vice versa (28–34). As clinical isolates of influenza A virus overwhelmingly include some percentage of filamentous virions and laboratory adaptation frequently results in the generation of strains with an exclusively spherical morphology (29, 34), an understanding of the biological relevance of filamentous influenza A virus particles has long been sought.

Hemagglutinin mediates attachment to host cells via binding to glycans possessing terminal sialic acid moieties and, following virion endocytosis, fusion between host and virion membranes (35). Neuraminidase has a complementary function to HA in that it is the receptor-destroying enzyme. NA cleaves sialic acids from host and virion surfaces to facilitate release of progeny virus (35). NA is also presumed to act on sialic acid-rich mucins that line target epithelia, which would otherwise prevent infection by competing with the cellular receptor for the HA binding site (36). Due to their opposing functions, the HA and NA proteins encoded by a given influenza virus are required to be in balance to achieve high viral fitness (37). A loss of HA/NA balance can occur through (i) reassortment involving either, but not both, of these genes (38); (ii) infection of a new tissue or host species, where sialic acids on cells or mucins may differ in type and distribution (39); (iii) a change in HA affinity/avidity due to the acquisition of antibody escape mutations (37, 40–42); or (iv) the presence of pharmaceutical neuraminidase inhibitors in the host (43). In each of these cases, studies have demonstrated that selective pressure on the virus can result in realignment of HA and NA functions such that viral attachment and release are not compromised. Typically, this realignment is achieved through direct modification of HA or NA. Observation of reassortant viruses suggests a greater level of complexity exists; however, alternative mechanisms for modulating HA-NA balance have not been explored in detail.

The HA and NA proteins have been found to be important to influenza virus transmission in a number of contexts (10, 44). Unexpectedly, the M segment was also found to be highly important to the transmissibility of the 2009 pandemic strain (9, 11, 12). Therefore, we formed the hypothesis that M1 and/or M2 proteins can alter HA/NA balance through effects on one or both glycoproteins. We tested this hypothesis through the examination of PR8-based viruses carrying combinations of the HA, NA, and/or M segments of the A/NL/602/09 (NL602) pandemic isolate. We confirmed that the M and NA gene segments of the NL602 virus contribute to transmissibility and also found a requirement for a cognate HA segment for optimal transmissibility. Among the reassortant viruses tested, efficient transmission among guinea pigs was found to correlate with increased neuraminidase activity. Surprisingly, changes to the M segment were sufficient to alter neuraminidase activity markedly, suggesting a mechanism by which M1 and/or M2 affects transmission. Finally, our data implicate changes to virion morphology as a mechanism by which M1 and/or M2 affects the functionality of NA.

MATERIALS AND METHODS

Ethics statement. This study was performed in accordance with the recommendations in the *Guide for the Care and Use of Laboratory Animals* of the National Institutes of Health (45). Animal husbandry and experimental procedures were approved by the Emory University Institutional Animal Care and Use Committee (IACUC protocol 2001001 071214GA).

Cells. Madin-Darby canine kidney (MDCK) cells were maintained in minimum essential medium (MEM) supplemented with 10% fetal bovine serum (FBS) and penicillin-streptomycin. 293T cells were maintained in Dulbecco's modified Eagle medium (DMEM) supplemented with 10% FBS. Human tracheobronchial epithelial (HTBE) cells were purchased from Lonza and cultured on transwell filters at an air-liquid interface with basal epithelial growth medium (BEGM) supplied to the basolateral chamber, essentially as directed by the manufacturer.

Guinea pigs. Female, Hartley strain guinea pigs weighing 300 to 350 g were obtained from Charles River Laboratories. Prior to intranasal inoculation, nasal lavage, or CO_2 euthanasia, guinea pigs were sedated with a mixture of ketamine and xylazine (30 and 2 mg/kg of body weight, respectively). Inoculation and nasal lavage were performed as described previously (46), with phosphate-buffered saline (PBS) as the diluent/collection fluid in each case.

Viruses. A/Puerto Rico/8/1934 (H1N1) (PR8)- and A/Netherlands/602/2009 (H1N1) (NL602)-based viruses were recovered by reverse genetics by following standard procedures (18, 47). Briefly, 8 plasmid rescue systems based on pDZ for PR8 and pHW for NL602 (48, 49) (a kind gift of Ron Fouchier) were used to transfect 293T cells. The pHW NL602 reverse genetic-derived clones were identical to the consensus sequence present in the original clinical specimen of virus (49). One day after transfection, 293T cells and associated medium were collected and injected into 9- to 11-day-old embryonated hens' eggs. Stock titers were determined by plaque assay on MDCK cells.

Immunostaining of plaques. Characterization of plaque phenotypes on MDCK cells was performed as described previously (50). For immunostaining, polyclonal guinea pig anti-PR8 serum (raised in house) was used as the primary antibody, horseradish peroxidase (HRP)-linked anti-guinea pig IgG (Invitrogen) was used as the secondary antibody, and TruBlue (KPL) peroxidase substrate was used for staining.

Multicycle growth experiments. MDCK cells were infected at a multiplicity of infection (MOI) of 0.002 PFU/cell. Following a 45-min incubation at 37°C, inoculum was removed and monolayers were washed with PBS. Dishes were then incubated at 37°C, and samples of growth medium were collected at 1, 12, 24, 48, and 72 h postinfection (hpi). Titers were determined by plaque assay on MDCK cells.

HTBE cells were washed with PBS to remove mucus and then infected at an MOI of 0.001 PFU/cell by adding virus in a 100-μl volume of PBS to the apical surface and incubating at 37°C for 45 min. The inoculum was then removed and the cells washed with PBS. At 1, 12, 24, 48, and 72 hpi, virus was collected from the apical surface of the cells by adding 200 μl PBS, incubating at 37°C for 30 min, and then transferring the 200 μl PBS to a tube. Titers were determined by plaque assay on MDCK cells.

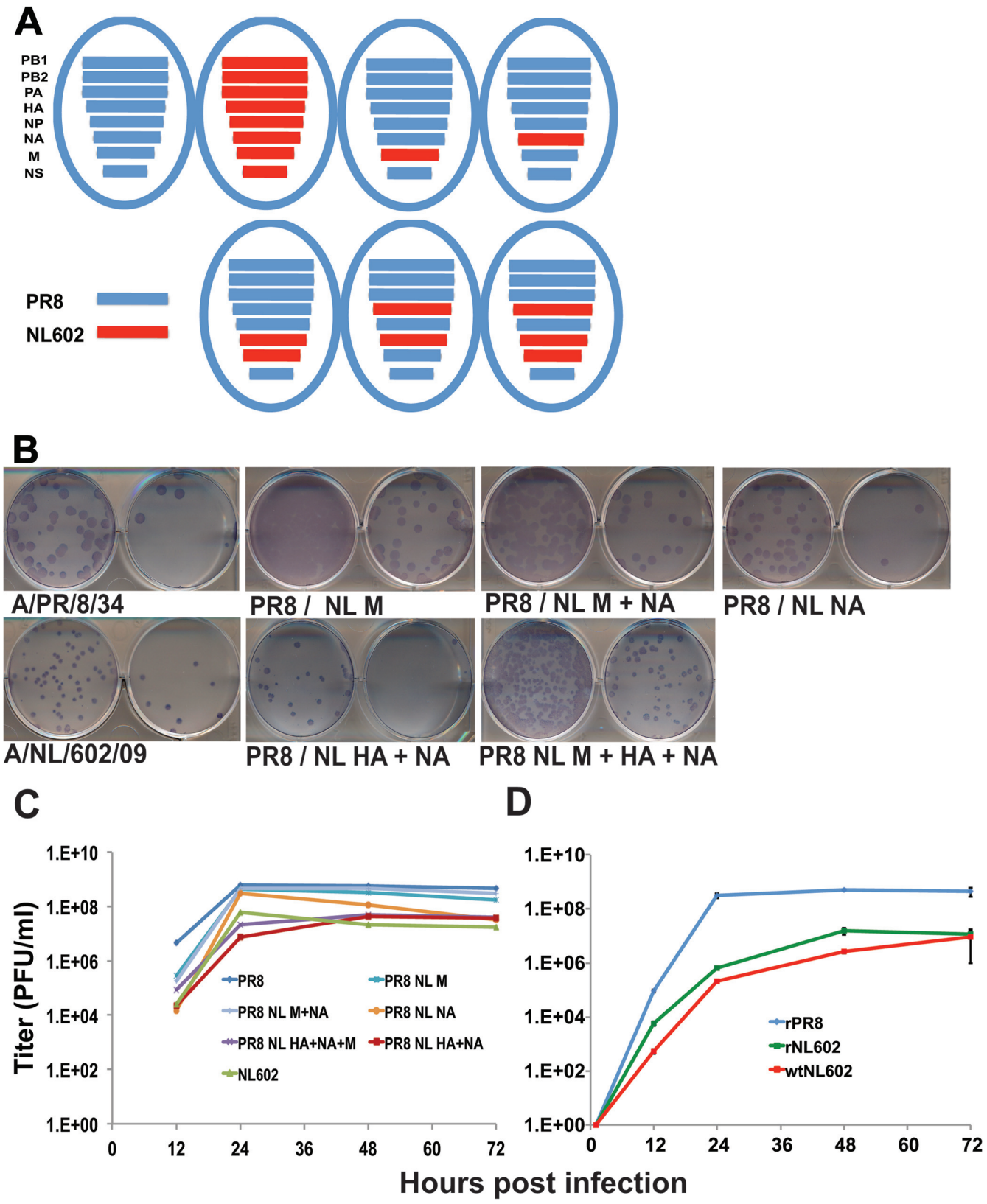

FIG 1 Schematic, plaque phenotype, and growth kinetics of rescued influenza viruses in MDCK cells. (A) Virus genotypes. Blue and red bars represent genes from A/PR/8/34 and A/NL/602/09 (NL602), respectively, as indicated. (B) Plaque phenotype of each virus (as indicated) was visualized at 48 h postinfection by immunostaining of infected MDCK cells. A polyclonal guinea pig serum reactive to PR8 virus was used to stain viral plaques. (C) MDCK cells were infected at a low MOI (0.002) with recombinant PR8, NL602, or PR8/NL602 reassortant viruses as indicated and incubated at 37°C in 5% CO_2 for 72 h. Released virus was enumerated by plaque assay of collected supernatants at the indicated time points. (D) MDCK cells were infected at a low MOI (0.002) with recombinant and wild-type NL602 viruses as indicated and treated as described for panel C.

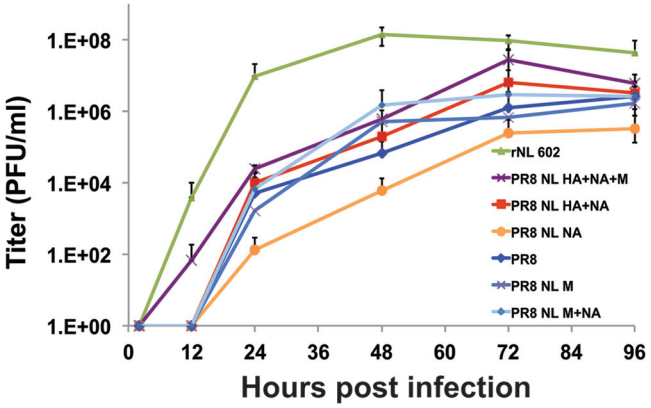

FIG 2 Growth kinetics of reassortant influenza viruses in differentiated HTBE cells. HTBE cells were infected at a low MOI (0.001) with recombinant PR8, NL602, or PR8/NL602 reassortant viruses (as indicated) and incubated at 37°C in 5% CO_2 for 96 h. Released virus was collected from the apical surface of differentiated cells and enumerated by plaque assay at the indicated time points.

Transmission experiments. To evaluate transmission, four guinea pigs were inoculated intranasally with 10^3 or 10^2 PFU of virus in 300 μl PBS. At 24 h postinoculation, each infected animal was placed in the same cage with one naive guinea pig. The four cages were then placed within an environmental chamber (Caron 6040) set to 20% relative humidity and 10°C. Standard rat cages with wire tops were used. Nasal washes were collected from all 8 guinea pigs on days 2, 4, 6, and 8 postinfection as previously described (46).

Electron microscopy. (i) TEM and scanning electron microscopy (SEM). For imaging of virions, MDCK cells were infected at an MOI of 5. Eighteen h postinfection, cells were fixed with 2.5% glutaraldehyde, post-fixed with 1% OsO_4 and 1.5% potassium ferrocyanide, rinsed with distilled water, and dehydrated through a series of ethanol washes. For transmission electron microscopy (TEM), monolayers were embedded in Eponate 12 resin, thin sectioned at 70 nm, and stained with 5% uranyl acetate and 2% lead citrate at the Emory Robert P. Apkarian Integrated Electron Microscopy Core. After sample preparation, grids were imaged using a Hitachi H-7500 transmission electron microscope and attached charge-coupled device (CCD).

For SEM, the chips underwent critical point drying in a Polaron E-3000 unit and were fixed to aluminum stubs, coated with 20 nm of

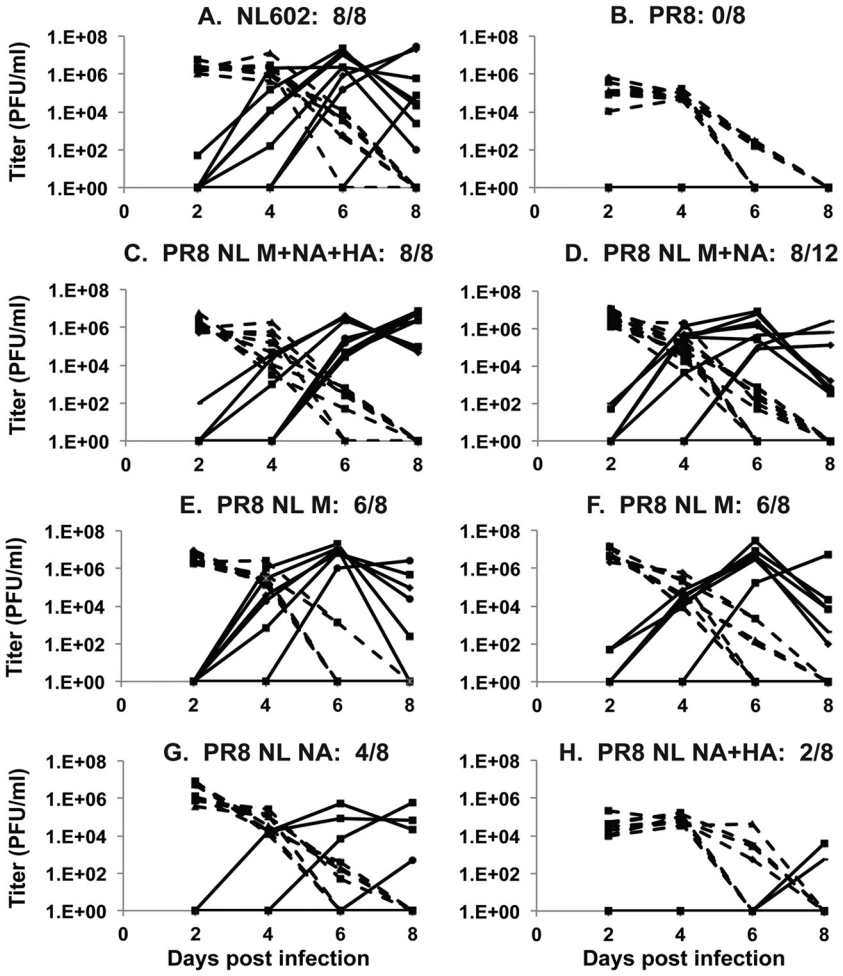

FIG 3 Growth kinetics and contact transmission of reassortant influenza viruses in guinea pigs. Guinea pigs were inoculated with 1,000 PFU of PR8, NL602, or PR8/NL602 reassortant viruses, as indicated, and viral titers in nasal wash, collected every 2 days postinfection from either inoculated (dashed lines) or contact-exposed (solid lines) animals, were determined by plaque assay. Each graph represents data from duplicate experiments, conducted at 10°C and 20% relative humidity, except one experiment in panel C, which was performed at 10°C and 75% relative humidity; in this case, all 4 exposed animals were infected on day 6 postinfection.

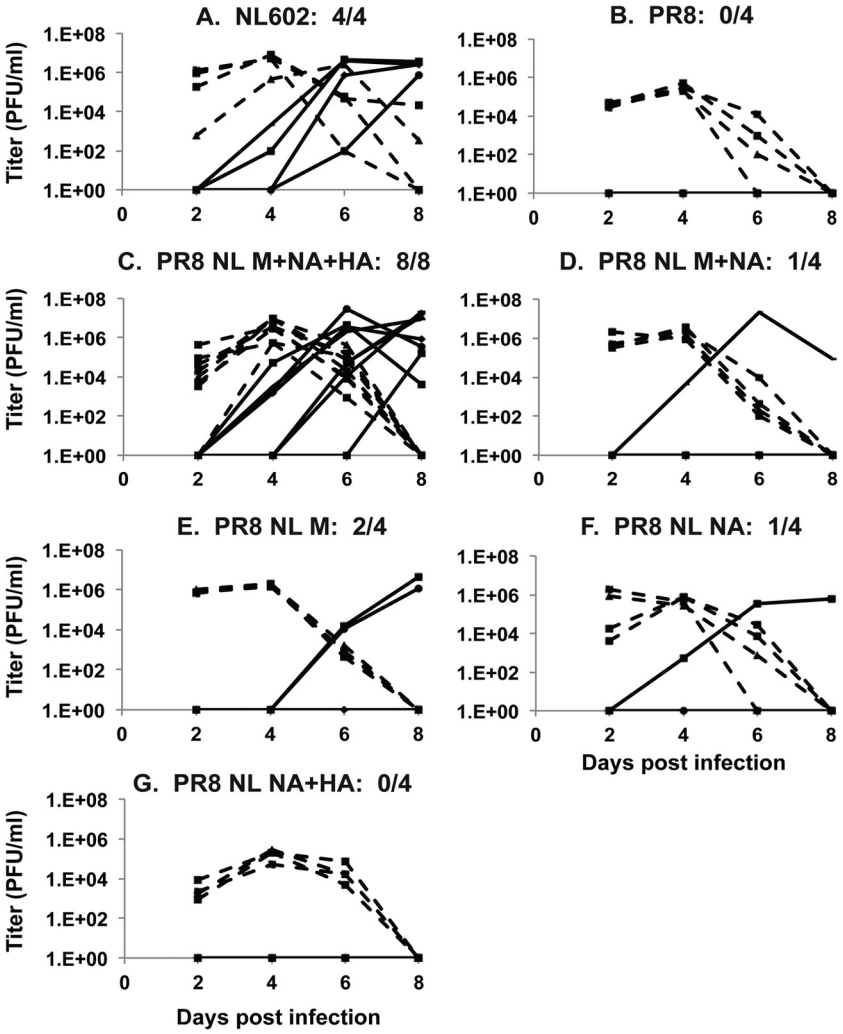

FIG 4 Growth kinetics and contact transmission of reassortant influenza viruses in guinea pigs. Guinea pigs were inoculated with 100 PFU of PR8, NL602, or PR8/NL602 reassortant viruses, as indicated, and viral titers in nasal wash, collected every 2 days postinfection from either inoculated (dashed lines) or contact-exposed (solid lines) animals, were determined by plaque assay.

chromium, and imaged using a Topcon DS130F scanning electron microscope.

Alternatively, to obtain negatively stained images of virions, 10-day-old embryonated eggs were infected with 1,000 PFU of the relevant virus. Forty-eight h postinfection, allantoic fluid was collected, and following sucrose cushion purification, virions were dialyzed and stained with 1% aqueous methyl tungstate at the Emory Robert P. Apkarian Integrated Electron Microscopy Core. After sample preparation, grids were imaged using a Hitachi H-7500 transmission electron microscope and attached CCD.

(ii) TEM particle counts. Virions within TEM fields were counted at a magnification of 30,000 to 40,000×. For each virus, between 178 and 845 virions (negatively stained TEM samples) and 53 and 239 virions (cell-associated virion TEM) were counted. Filaments were defined as being equal to or greater than 300 nm in length, and no more than 200 nm in cross section, along 90% of the virion length. Virions shorter than 300 nm in length were defined as spheres. From these counts, the percentage of spherical and filamentous virions was calculated. The difference in proportions test was used to determine if the proportion of virions that were filamentous was significantly different from that of the wild type. Results were considered significant if $P < 0.05$.

Neuraminidase activity. To assess the neuraminidase activity associated with each virus, enzyme kinetic data on each virus was obtained essentially as described by Peiris and coworkers (10). Briefly, neuraminidase kinetics were determined by incubation of virus preparations with the fluorogenic sialoside MUNANA at final concentrations of 1.12 to 150 μM in a total volume of 100 μl. Fluorescence was detected using a BioTek Synergy H1 plate reader every minute for 1 h, and the linear slopes of the resultant fluorescence curves were fit to the Michaelis-Menten nonlinear regression algorithm for enzyme kinetics modeling. Virus input concentrations were normalized to PFU and confirmed to be of approximately equal numbers of virions by NP RNA copy number, as determined by quantitative reverse transcription-PCR (qRT-PCR) of extracted viral RNA.

RESULTS

***In vitro* characterization of recombinant viruses.** Using reverse genetics, a set of seven reassortant viruses was generated. The set comprised the recombinant wild-type PR8 (rPR8) and NL602 viruses and five reassortants thereof: PR8 NL602 M, PR8 NL602 NA, PR8 NL602 M+NA, PR8 NL602 HA+NA, and PR8 NL602 M+NA+HA (Fig. 1A). Initial characterization of these viruses was performed in MDCK cells. Plaque assays showed clear plaques for all of the recombinant viruses: those carrying the NL602 HA

segment (including the wild-type rNL602 virus) were found to form smaller plaques than viruses carrying the PR8 HA segment (Fig. 1B). All recombinant viruses also replicated well in multicycle growth experiments in MDCK cells (Fig. 1C). Mirroring the trend in plaque morphologies, the rPR8 virus grew to the highest titers and the rNL602 virus grew to the lowest titers from a low multiplicity of infection (MOI). Although the differences among the reassortant strains were small, the MDCK growth phenotypes appeared to map to the HA segment. To confirm that the recombinant NL602 virus was not attenuated due to artifactual errors in the genome, its growth in MDCK cells was compared to that of the biological NL602 isolate (Fig. 1D). The results indicated similar growth for rNL602 and biological NL602 viruses, with the titers of the biological NL602 being slightly lower (perhaps due to some components of this quasispecies).

Viral growth was then assessed in a more relevant substrate: fully differentiated human tracheobronchial epithelial (HTBE) cells cultured at the air-liquid interface. In this system, the rNL602 virus showed very robust growth (peaking at 1.4×10^8 PFU/ml after 48 h), and the laboratory-adapted rPR8 strain showed relatively poor growth (100- to 1,000-fold lower titers than rNL602 virus) (Fig. 2). The growth of the PR8-NL602 reassortant viruses bracketed that of rPR8 virus: of this group, the PR8 NL602 M+NA+HA virus showed the most efficient growth and the two strains carrying the NL602 NA but the PR8 HA grew very poorly, presumably due to an HA-NA imbalance. It is interesting, however, that the inclusion of the NL602 M with the NL602 NA enhanced growth over the single-gene reassortant with only the NL602 NA segment.

Growth and contact transmission in the guinea pig model. In the guinea pig model, the wild-type rNL602 virus transmits with high efficiency (Fig. 3A and 4A) (51, 52), while the wild-type rPR8 strain does not transmit (Fig. 3B and 4B) (9). With the aim of understanding the contribution of the pandemic M, NA, and HA segments to the transmissible phenotype of rNL602 virus, the transmissibility of the five PR8-NL602 reassortant viruses was evaluated in a guinea pig contact model. As shown in Fig. 3C, at an inoculum dose of 1,000 PFU, the fully transmissible phenotype of rNL602 virus was recapitulated by inclusion of the pandemic M, NA, and HA segments in the PR8 background. Consistent with the previous report of Chou et al. (9), we found that inclusion of only the NL602 M segment in the PR8 background also led to a marked improvement in transmission: with 16 transmission pairs, this virus transmitted to 75% of contact guinea pigs (Fig. 3E and F). A critical role for the NL602 M segment was further confirmed by the efficient transmission of the PR8-based virus containing M and NA segments from NL602, which transmitted to 8 out of 12 contact animals (Fig. 3D), as well as by the poor transmission of the PR8 and PR8 NL602 HA+NA viruses (Fig. 3B and H). The PR8 NL602 NA virus transmitted to four out of eight animals (Fig. 3G). In addition to increased transmissibility, the inclusion of the pandemic M segment, NA segment, or both segments significantly improved growth ($P > 0.05$) of the PR8-based viruses (as assayed on day two postinfection) relative to the parental rPR8.

The ability of the viruses to transmit from a lower inoculation dose of 100 PFU next was examined in the guinea pig model. Under these more stringent conditions, the PR8 NL602 M+NA+HA virus was again found to transmit efficiently (Fig. 4C), while the PR8 NL602 M+NA, PR8 NL602 M, and PR8 NL602 NA viruses each retained the ability to replicate and transmit (Fig. 4D and E), albeit with reduced efficiency relative to the PR8 NL602 M+NA+HA virus. In contrast, the PR8 and PR8 NL602 HA+NA viruses failed to transmit at this inoculum dose (Fig. 4B and G).

TABLE 1 Virions possessing the PR8 M segment have lower V_{max}, but not K_m, of NA interaction with MUNANA than virions possessing NL602 M

Virus and input[a] (PFU)	V_{max}[b] (SE; 95% CI)	K_m (SE; 95% CI)
PR8		
1×10^6	1,798 (72.1; 1,645–1,950)	8.1 (1.4; 5.2–11.1)
	1,807 (55.7; 1,687–1,926)	9.9 (1.1; 7.5–12.2)
	1,908 (52.7; 1,794–2,021)	10.8 (1.1; 8.5–13.1)
PR8/NL M		
1×10^6	2,621 (67.3; 2,476–2,765)	10.8 (1.0; 8.7–12.9)
	2,568 (73.0; 2,411–2,724)	11.2 (1.1; 8.7–13.5)
	2,749 (73.1; 2,592–2,905)	11.6 (1.1; 8.9–13.4)
PR8/NL HA+NA[c]		
1×10^5	1,407 (31.4; 1,304–1,475)	28.2 (1.8; 24.4–32.0)
	1,472 (40.3; 1,386–1,556)	29.3 (2.2; 24.5–34.0)
	1,618 (22.1; 1,499–1,738)	22.1 (2.7; 16.3–27.8)
PR8/NL M+NA+HA[c]		
1×10^5	2,354 (75.5; 2,192–2,516)	24.7 (2.3; 19.8–29.7)
	2,296 (74.4; 2,136–2,455)	23.3 (2.2; 18.5–28.1)
	2,266 (90.9; 2,073–2,458)	18.8 (2.8; 13.0–24.7)

[a] Presence of equal numbers of virions was confirmed by measuring NP RNA copy number using qRT-PCR. No significant difference in copy number was observed between PR8 and PR8/NL M virus preparations or between PR8/NL HA+NA and PR8/NL M+NA+HA virus preparations in independent experiments.
[b] Enzyme kinetics data were fit to the Michaelis-Menten equation by nonlinear regression to determine the Michaelis constant (K_m) and maximum velocity (V_{max}) of substrate conversion. CI, confidence interval. SE, standard errors. For each virus, data are presented from three independent experiments.
[c] Note that the NA proteins of PR8 NL09 HA+NA and PR8 NL09 HA+NA+M differ from the NA carried by PR8 and PR8 NL09 M; thus, the NL09 NA-containing viruses should only be compared to each other.

Neuraminidase activity of reassortant viruses. As neuraminidase activity has been reported to be important to the transmissibility of influenza virus in guinea pigs (53, 54), we wished to test whether the NA activity of the transmissible viruses differed from those of the nontransmissible strains. Since the M segment is central to the transmissible phenotype, we focused on viruses that differ genetically only in the M segment. Two subsets of viruses, each possessing the same NA segment, were compared: (i) PR8 versus PR8 NL602 M virus and (ii) PR8 NL602 HA+NA versus PR8 NL602 M+NA+HA virus. In each case, inclusion of the pandemic M segment in place of the PR8 M segment was found to increase the neuraminidase activity associated with a standardized quantity of virions (Table 1). The sequence of each NA segment was verified to confirm that the observed changes in neuraminidase V_{max} were not due to mutations that had arisen in the NA segment. In addition, while the V_{max} of preparations possessing the pandemic M segment were increased relative to those possessing the PR8 M segment, the K_m was similar, suggesting no change in affinity of the neuraminidase protein for substrate. The increased V_{max} of viruses possessing the pandemic M segment suggests a mechanism through which M1 and/or M2 could alter virus fitness and transmission.

Morphology of reassortant viruses. We next wished to ad-

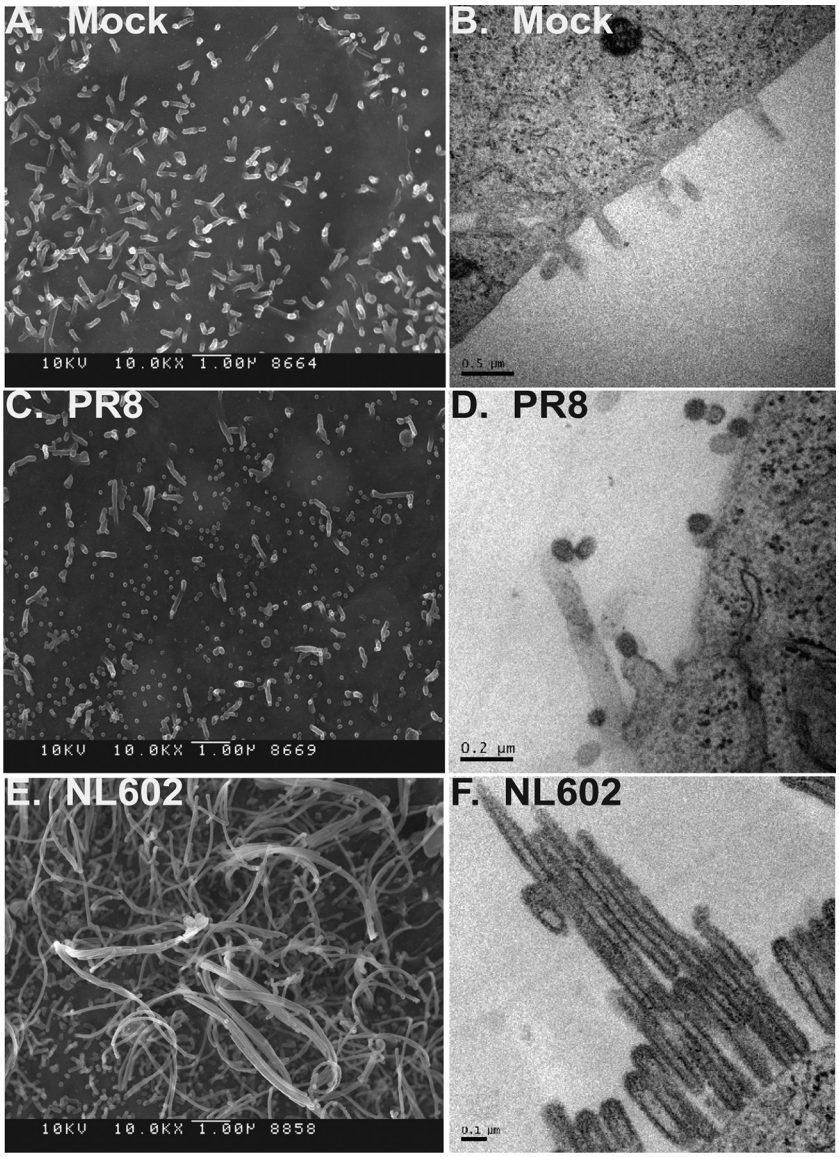

FIG 5 PR8 and NL602 viruses display distinct virion morphologies. Virion morphologies are shown as SEM (A, C, and E) or TEM (B, D, and F) images of well-bound MDCK cells that were infected at an MOI of 5.0 and mock incubated or incubated with virus for 16 h before fixing and staining. (A and B) Mock-infected MDCK cells display distinctive filopodia. PR8 virus is visible as spherical virions of 100 to 200 nm in diameter (C and D), while NL602 virus produced pleiomorphic virions, including highly filamentous examples (E and F).

dress the mechanism by which M1 and/or M2 affects NA activity. Since spherical and filamentous virus particles differ greatly in the surface area of the (neuraminidase-containing) viral envelope, we hypothesized that changes to virion shape are associated with changes to virion-associated neuraminidase activity; therefore, we examined the morphology of virus particles produced by each virus in our panel. As expected based on previous reports (29, 55), the rPR8 virus produced spherical or small ovoid particles almost exclusively (Fig. 5C and D). Also consistent with published data on 2009 pandemic strains (34, 56), the rNL602 virus was highly filamentous (Fig. 5E and F), particularly when imaged associated with a cell monolayer. Negative-stain transmission electron microscopy of released rNL602 virus, concentrated through ultracentrifugation with a sucrose cushion, revealed a wide range of virion shapes, including filaments and spheres. While it is typical, even for a filamentous influenza virus, to see spherical virions by this method (32), the larger spheres and irregular shapes observed most likely are cellular debris and filaments that were damaged during preparation of the concentrated sample. Imaging of the PR8 NL602 M+NA+HA virus by cell-associated transmission electron microscopy revealed robust filament formation, similar to that seen with the rNL602 virus (compare Fig. 6A and B to 5E and F). When the NL602 M segment alone was included in the PR8 background, filamentous virus particles were produced (Fig. 6C and D), but to relatively lower levels of prevalence than the PR8 NL602 M+NA+HA reassortant ($P > 0.05$ by difference of proportions test). Interestingly, the NL602 NA alone was also found to confer a partially filamentous morphology to the PR8-based virus, PR8 NL602 NA (Fig. 6E and F). In contrast, while the PR8 HA+NA virus produced a number of filaments, these were typi-

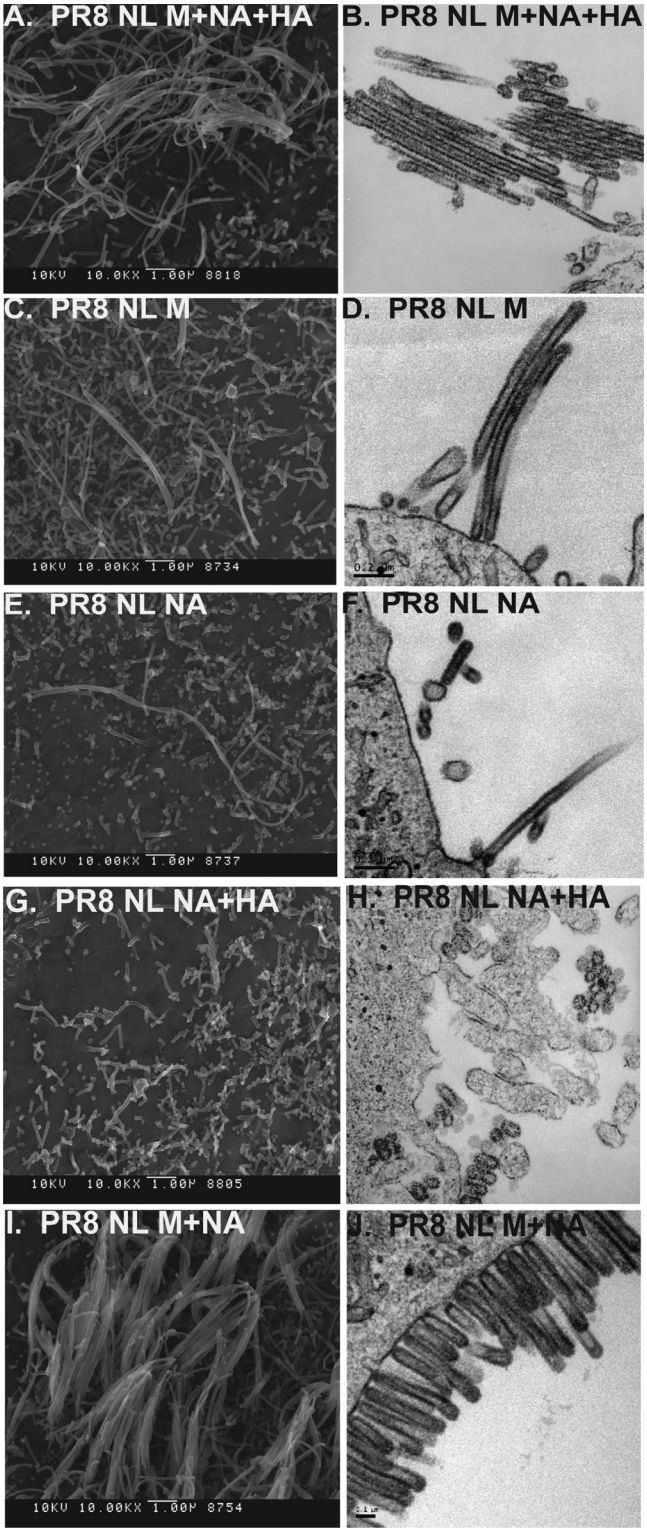

FIG 6 PR8/NL M+NA+HA virus recapitulates the virion morphology of rNL602 virus. Virion morphologies are shown as SEM (A, C, E, G, and I) or TEM images (B, D, F, H, and J) of well-bound MDCK cells that were infected at an MOI of 5.0 and incubated with the indicated viruses for 16 h before fixing and staining. PR8/NL M+NA+HA virus exhibits long filaments, as well as spheres, similar to the rNL602 virus (compare panels A and B to Fig. 5E and F). Other reassortant viruses display various rates of prevalence of filamentous particles.

cally shorter in length than the PR8 NL602 NA virus (Fig. 6G to H and Table 2).

The relative proportions of spherical (<300 nm) and filamentous (>300 nm) virions produced by each virus, as visualized by negative-stain TEM of released virus (Fig. 7) and TEM of infected MDCK cells, are summarized in Table 2. The results of these size-based particle counts clearly show quantitative differences among the virus strains in the prevalence of filaments.

In summary, the NL602 M and NA segments individually, or in combination, conferred various degrees of filamentous virion morphology to PR8 virus. The M, NA, and HA segments from NL602 together generated a morphological phenotype which was highly similar to that of the full-length wild-type NL602 virus. Of significant interest, a strong correlation between the prevalence of filamentous particles greater than 300 nm and efficiency of contact transmission was observed (Table 2). Thus, our data suggest a model in which pandemic M1 and/or M2 leads to increased virion-associated NA activity on a per-virion basis and, as a result, heightened transmissibility by favoring the production of longer filamentous virions than the parental PR8.

DISCUSSION

We have shown that a recombinant PR8-based influenza virus, possessing the M, NA, and HA gene segments from the pH1N1 strain A/NL/602/09, is capable of efficient contact transmission in the guinea pig model from low-dose inoculation. This transmission was indistinguishable from that of wild-type recombinant A/NL/602/09 virus. Consistent with previously published data (9), our evaluation of single-gene reassortants indicated that the M segment of the pandemic strain is critical, and the NA segment of the pandemic strain contributes independently to the transmission of a PR8-based virus in the guinea pig model. Interestingly, wild-type NL602 virus and the PR8 NL M+NA+HA virus retained optimally efficient transmission among guinea pigs upon reduction of the inoculation dose to 100 PFU. In contrast, the PR8 NL M, PR8 NL M+NA, and PR8 NL NA viruses demonstrated decreased transmission under these more stringent conditions, suggesting that each of the HA, NA, and M segments derived from NL602 contribute to the optimal transmission of the PR8-based virus. Neither the PR8 nor the PR8 NL HA+NA virus was transmitted from guinea pigs infected at 100 PFU. Examination of transmission from low dose is a valuable experimental tool for dissecting relative transmission efficiencies. In addition, we suggest that this assay is biologically relevant: the ability of a virus to transmit efficiently from a host infected at a low dose would be a highly advantageous biological trait, likely conferring an important selective advantage at a population level.

Of note, Ma and colleagues (12) have shown that, in a swine influenza virus background, strains individually possessing either the 2009 pandemic M or NA segment grew to lower titers than parental virus, either *in vitro* (in MDCK cells) or following intratracheal inoculation of swine at a dose of 10^6 50% egg infectious doses (EID_{50}). However, in each substrate, the reassortant strain containing both the M and NA segments replicated to higher titers than the parental swine virus. *In vivo*, the M+NA virus also subsequently transmitted among swine. A virus possessing pandemic M, NA, and HA segments in the parental background was not tested in that study.

The level of neuraminidase activity exhibited by particular influenza virus strains has been shown to affect transmission effi-

TABLE 2 Reassortant viruses differ in prevalence of filamentous virions

Morphology and particle length (nm)	Virus prevalence[a] (%)													
	rPR8		PR8/NL HA+NA		PR8/NL NA		PR8/NL M+NA		PR8/NL M		PR8/NL M+NA+HA		rNL602	
	NS	TEM	NS	TEM	NS	TEM	NS	TEM	NS	TEM	NS	TEM	NS	TEM
Spherical														
<100	6.5	75.5	8.9	53.8	9.6	47.9	1.8	16.7	2.7	42.4	4.9	44.8	24.2	20.9
100–200	80.6	24.5	67.1	42.4	65.3	32.9	57.4	27.2	75.2	43.0	53.2	14.7	47.8	31.8
200–300	9.5	0	17.1	1.6	15.7	9.6	26.4	15.5	14.0	4.1	13.1	11.0	16.9	12.2
All sizes	96.6	100	93.0	100	90.6	90.4	85.6	59.4	91.9	89.5	71.1	70.6	88.8	64.9
Filamentous														
300–500	3.2	0	4.9	2.2	7.0	2.7	9.8	25.5	5.3	2.3	16.7	8.6	2.8	27.7
500–1,000	0.2	0	1.9	0	2.4	6.8	3.4	14.2	2.3	4.7	6.4	16.6	5.1	4.7
>1,000	0	0	0.2	0	0	0	1.2	0.8	0.5	3.5	5.8	4.3	3.4	2.7
All sizes	3.4[b]	0	7.0[b]	2.2[b]	9.4[b]	9.6[b]	14.4[b]	40.6	8.1[b]	10.5[b]	28.9	29.4	11.2[b]	35.1
Total no. of particles	845	53	428	184	510	73	326	239	786	172	329	163	178	148
Total % transmission efficiency in GP[c]	0		17		42		56		70		100		100	

[a] NS, negative-stain TEM of released virus; TEM, TEM of infected, sectioned MDCK cells.
[b] Percentage of filamentous virions (>300 nm in length) is significantly different ($P > 0.05$) from that of PR8/NL M+NA+HA by difference of proportions test.
[c] Combined results of contact transmission experiments involving guinea pigs (GP) inoculated at either 100 or 1,000 PFU and naive cagemates.

ciency in both guinea pig and ferret models (57). In addition to the observation that HA/NA balance is critical for the transmission of the 2009 pandemic virus (10), a number of research groups have demonstrated that mutations that confer resistance to NA inhibitors and reduce the NA activity of the virus also resulted in decreased transmission (53, 54). These resistance mutations can affect both the replication and transmission of influenza viruses carrying them (58, 59). In some cases, however, viruses possessing NA inhibitor-resistant phenotypes nonetheless transmit efficiently, and permissive changes elsewhere in the NA gene (60), as well as the overall gene constellation, appear to play a role in supporting transmission of these viruses (57).

We have also found that transmission correlates with increased NA activity. Interestingly, this trend is clear even between virus pairs that carry identical NA genes and differ only in their M segment. Thus, we have shown that the NA activity of influenza virus particles is dependent on the M segment. We suggest that this effect is mediated through virion morphology and that transmission, NA activity, and virion morphology are linked.

It is not conclusive from our data that the observed increases in NA activity conferred by the inclusion of the NL602 M segment, in place of the PR8 M, are biologically relevant. It is possible that as the NA activity increases, presumably through increased incorporation of NA, a concomitant increase in HA molecules results in particles that maintain an overall balance between HA and NA. However, we have not assessed incorporation levels of HA or NA in the virions biochemically, and our data do not allow us to assess whether levels of virion-incorporated HA and NA increase proportionately as the virion length increases. Furthermore, it is possible that proportionate changes in the levels of HA and NA would not be "functionally colinear," such that increases in avidity due to increased levels of virion-associated HA occur at a different rate than increases in receptor cleavage efficiency. These aspects of the virion biology remain to be investigated.

Among the viruses on our panel, strains producing long filamentous virions tended to transmit more efficiently among guinea pigs. Wild-type A/PR/8/34 virus, which is almost exclusively spherical, did not transmit. PR8/NL HA+NA virus possesses mainly short filamentous or spherical virions and transmitted inefficiently. The inclusion of the NL602 M segment in the PR8 virus, which increased replication of the resultant virus *in vivo* and conferred 75% transmission at 1,000 PFU, also altered the proportion of virions longer than 1 μm, from 0% in PR8 to 3.5% in PR8 NL M, as assessed by measurement of TEM images. The largely filamentous PR8 NL M+NA+HA and wild-type NL602 virions possess 4.3% and 2.7% of filaments greater than 1 μm in length (as assessed by TEM), respectively, and both transmitted efficiently, even from an inoculation dose of 100 PFU. While we did not observe a strong correlation between shedding titers and transmission efficiency, those viruses that transmitted least efficiently (PR8 and PR8 NL NA+HA) were shed to markedly lower titers than the remaining viruses.

A recent report by Subbarao and colleagues (11) involving reassortant virus strains possessing pH1N1 M and NA segments also supports a role for morphological changes in determining transmissibility. In that study, replacement of the pandemic M and NA segments with those from a swine-adapted virus resulted in a loss of respiratory droplet transmissibility from ferrets inoculated intranasally at $10^{6.5}$ 50% tissue culture infectious doses ($TCID_{50}$). This nontransmissible strain also exhibited a spherical morphology.

In trying to understand how the M segment impacts transmissibility, our data do not allow us to separate the effects of M on morphology and NA activity. Nevertheless, we favor a model in which changes to morphology allow modulation of NA activity and, in turn, transmissibility over the alternative model in which virion shape is an independent determinant of transmission.

Several previous studies have demonstrated that the gene products of the M segment affect the morphology of the influenza virion (28, 29, 31, 32). Elleman and Barclay (29) reported that differences in morphology between (i) the laboratory-adapted strains A/PR/8/34 and A/WSN/33 and (ii) the human isolate

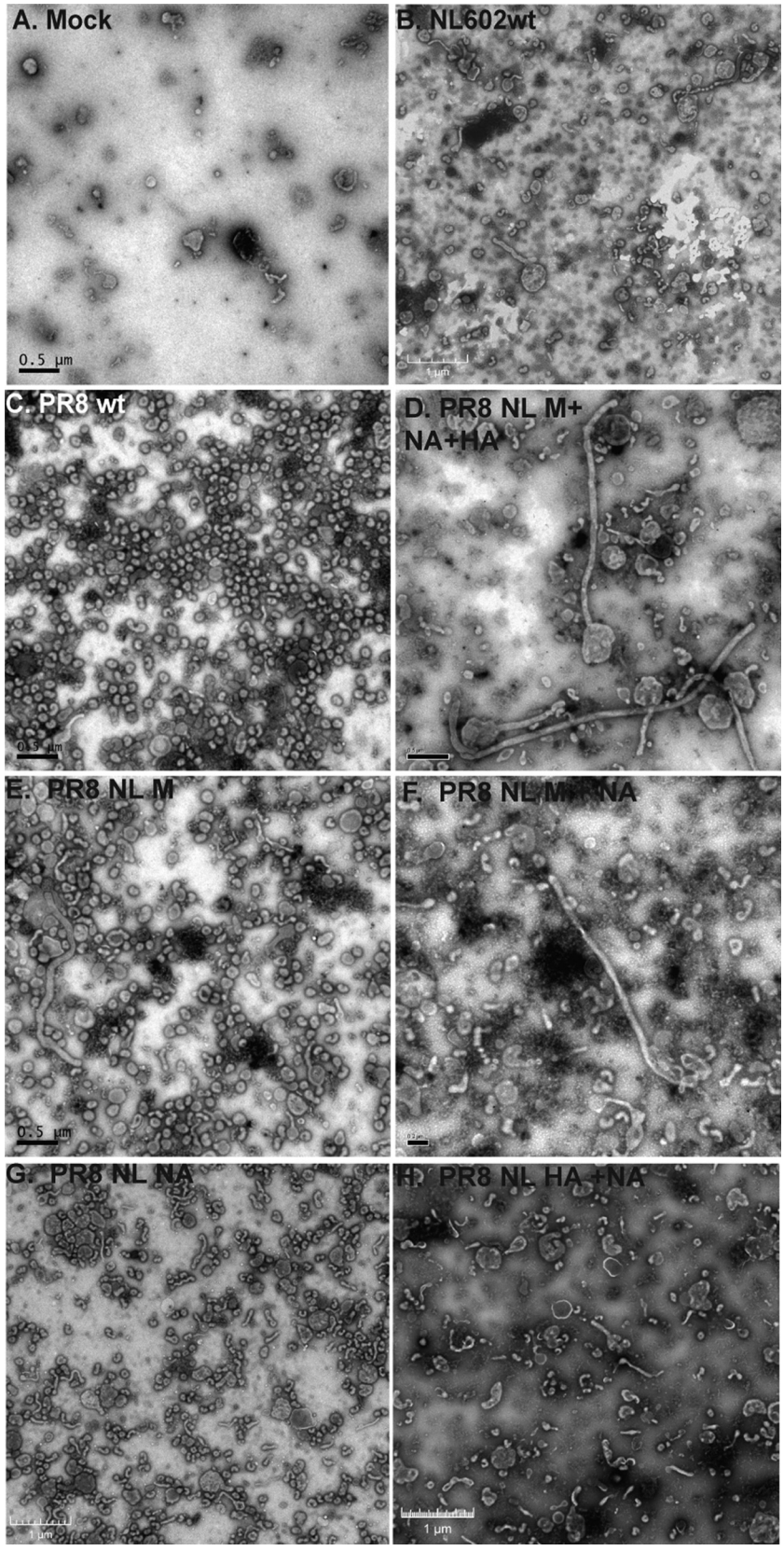

FIG 7 PR8/NL M+NA+HA recapitulates the virion morphology of rNL602 virus. Virion morphologies shown as negative-stain images of influenza virions, as indicated, grown in embryonated chicken egg for 48 h and concentrated through sucrose-cushioned centrifugation before fixing and staining.

A/Victoria/3/75 could be mapped to the matrix protein, in particular M1 residues 41, 95, and 218. Similarly, Bourmakina and Garcia-Sastre (28) identified M1 residues 95 and 204 as morphology determinants. Roberts and colleagues reported that amino acids in both the matrix and M2 proteins affect virion morphology (32), again including M1 residue 41.

The matrix proteins of PR8 and NL602 have 13 amino acid differences (95% identity), while the M2 proteins of the strains differ by 14 amino acids (86% identity). We have not mapped the specific residues that are responsible for the observed phenotypes in the present study, but among the changes, M1 residue 41, as well as residues 207, 209, and 214 (which map close to residue 218, also identified by Elleman and Barclay [29]), differ between the PR8 and NL602 strains.

The NA protein of influenza virus has been reported to interact with the M1 protein through its cytoplasmic tail and transmembrane regions (61, 62). Furthermore, Mitnaul and colleagues (63) have shown that deletion of the NA cytoplasmic tail can alter the morphology of influenza virions, suggesting that NA-M1 interaction affects morphology. Notably, no amino acid differences exist in the NA cytoplasmic tail domains of PR8 and NL602, suggesting that amino acid residues in the transmembrane domain of NA are responsible for the changes in morphology observed upon replacement of the PR8 NA with that of NL602. There are 8 amino acid polymorphisms between the two transmembrane domains, as well as additional differences present in the membrane-proximal stalk region of the two proteins.

In sum, our data reveal a previously unappreciated mechanism through which the M segment can tune the receptor-destroying activity of influenza virus. We suggest that M1- or M2-mediated changes to morphology could alter NA V_{max} through alterations in NA incorporation, distribution, or presentation at the virion surface. We also show that cognate (NL602) M, NA, and HA segments confer more efficient transmissibility than a matched (PR8) HA and NA combined with the NL602 M segment. The M-NA functional interaction we describe appears to underlie the prominent role of the 2009 pandemic M segment in supporting efficient transmission and may be a highly important means by which influenza viruses restore HA/NA balance following reassortment or transfer to new host environments.

ACKNOWLEDGMENTS

We are grateful to Ron Fouchier for the A/Netherlands/602/2009 (H1N1) virus and reverse genetics system pHW NL602. We also appreciate the work of Hong Yi and Jeannette Taylor of the Robert P. Apkarian Integrated Electron Microscopy Core for TEM and SEM sample processing.

We thank the Georgia Research Alliance for support to J.S. and A.C.L. through equipment grants. This work was funded by the Centers for Excellence in Influenza Research and Surveillance (CEIRS), contract number HHSN266200700006C.

REFERENCES

1. **Dacso CC, Couch RB, Six HR, Young JF, Quarles JM, Kasel JA.** 1984. Sporadic occurrence of zoonotic swine influenza virus infections. J. Clin. Microbiol. **20:**833–835.
2. **de Jong JC, de Ronde-Verloop JM, Bangma PJ, van Kregten E, Kerckhaert J, Paccaud MF, Wicki F, Wunderli W.** 1986. Isolation of swine-influenza-like A(H1N1) viruses from man in Europe, 1986. Lancet **ii:** 1329–1330.
3. **Gregory V, Bennett M, Thomas Y, Kaiser L, Wunderli W, Matter H, Hay A, Lin YP.** 2003. Human infection by a swine influenza A (H1N1) virus in Switzerland. Arch. Virol. **148:**793–802. http://dx.doi.org/10.1007/s00705-002-0953-9.
4. **Rota PA, Rocha EP, Harmon MW, Hinshaw VS, Sheerar MG, Kawaoka Y, Cox NJ, Smith TF.** 1989. Laboratory characterization of a swine influenza virus isolated from a fatal case of human influenza. J. Clin. Microbiol. **27:**1413–1416.
5. **Wells DL, Hopfensperger DJ, Arden NH, Harmon MW, Davis JP, Tipple MA, Schonberger LB.** 1991. Swine influenza virus infections. Transmission from ill pigs to humans at a Wisconsin agricultural fair and subsequent probable person-to-person transmission. JAMA **265:**478–481.
6. **Myers KP, Olsen CW, Gray GC.** 2007. Cases of swine influenza in humans: a review of the literature. Clin. Infect. Dis. **44:**1084–1088. http://dx.doi.org/10.1086/512813.
7. **Garten RJ, Davis CT, Russell CA, Shu B, Lindstrom S, Balish A, Sessions WM, Xu X, Skepner E, Deyde V, Okomo-Adhiambo M, Gubareva L, Barnes J, Smith CB, Emery SL, Hillman MJ, Rivailler P, Smagala J, de Graaf M, Burke DF, Fouchier RA, Pappas C, Alpuche-Aranda CM, Lopez-Gatell H, Olivera H, Lopez I, Myers CA, Faix D, Blair PJ, Yu C, Keene KM, Dotson PD, Jr, Boxrud D, Sambol AR, Abid SH, St George K, Bannerman T, Moore AL, Stringer DJ, Blevins P, Demmler-Harrison GJ, Ginsberg M, Kriner P, Waterman S, Smole S, Guevara HF, Belongia EA, Clark PA, Beatrice ST, Donis R, Katz J, Finelli L, Bridges CB, Shaw M, Jernigan DB, Uyeki TM, Smith DJ, Klimov AI, Cox NJ.** 2009. Antigenic and genetic characteristics of swine-origin 2009 A(H1N1) influenza viruses circulating in humans. Science **325:**197–201. http://dx.doi.org/10.1126/science.1176225.
8. **Smith GJ, Vijaykrishna D, Bahl J, Lycett SJ, Worobey M, Pybus OG, Ma SK, Cheung CL, Raghwani J, Bhatt S, Peiris JS, Guan Y, Rambaut A.** 2009. Origins and evolutionary genomics of the 2009 swine-origin H1N1 influenza A epidemic. Nature **459:**1122–1125. http://dx.doi.org/10.1038/nature08182.
9. **Chou YY, Albrecht RA, Pica N, Lowen AC, Richt JA, Garcia-Sastre A, Palese P, Hai R.** 2011. The M segment of the 2009 new pandemic H1N1 influenza virus is critical for its high transmission efficiency in the guinea pig model. J. Virol. **85:**11235–11241. http://dx.doi.org/10.1128/JVI.05794-11.
10. **Yen HL, Liang CH, Wu CY, Forrest HL, Ferguson A, Choy KT, Jones J, Wong DD, Cheung PP, Hsu CH, Li OT, Yuen KM, Chan RW, Poon LL, Chan MC, Nicholls JM, Krauss S, Wong CH, Guan Y, Webster RG, Webby RJ, Peiris M.** 2011. Hemagglutinin-neuraminidase balance confers respiratory-droplet transmissibility of the pandemic H1N1 influenza virus in ferrets. Proc. Natl. Acad. Sci. U. S. A. **108:**14264–14269. http://dx.doi.org/10.1073/pnas.1111000108.
11. **Lakdawala SS, Lamirande EW, Suguitan AL, Jr, Wang W, Santos CP, Vogel L, Matsuoka Y, Lindsley WG, Jin H, Subbarao K.** 2011. Eurasian-origin gene segments contribute to the transmissibility, aerosol release, and morphology of the 2009 pandemic H1N1 influenza virus. PLoS Pathog. **7:**e1002443. http://dx.doi.org/10.1371/journal.ppat.1002443.
12. **Ma W, Liu Q, Bawa B, Qiao C, Qi W, Shen H, Chen Y, Ma J, Li X, Webby RJ, Garcia-Sastre A, Richt JA.** 2012. The neuraminidase and matrix genes of the 2009 pandemic influenza H1N1 virus cooperate functionally to facilitate efficient replication and transmissibility in pigs. J. Gen. Virol. **93:**1261–1268. http://dx.doi.org/10.1099/vir.0.040535-0.
13. **Sorrell EM, Wan H, Araya Y, Song H, Perez DR.** 2009. Minimal molecular constraints for respiratory droplet transmission of an avian-human H9N2 influenza A virus. Proc. Natl. Acad. Sci. U. S. A. **106:**7565–7570. http://dx.doi.org/10.1073/pnas.0900877106.
14. **Tumpey TM, Maines TR, Van Hoeven N, Glaser L, Solorzano A, Pappas C, Cox NJ, Swayne DE, Palese P, Katz JM, Garcia-Sastre A.** 2007. A two-amino acid change in the hemagglutinin of the 1918 influenza virus abolishes transmission. Science **315:**655–659. http://dx.doi.org/10.1126/science.1136212.
15. **Herfst S, Schrauwen EJ, Linster M, Chutinimitkul S, de Wit E, Munster VJ, Sorrell EM, Bestebroer TM, Burke DF, Smith DJ, Rimmelzwaan GF, Osterhaus AD, Fouchier RA.** 2012. Airborne transmission of influenza A/H5N1 virus between ferrets. Science **336:**1534–1541. http://dx.doi.org/10.1126/science.1213362.
16. **Imai M, Watanabe T, Hatta M, Das SC, Ozawa M, Shinya K, Zhong G, Hanson A, Katsura H, Watanabe S, Li C, Kawakami E, Yamada S, Kiso M, Suzuki Y, Maher EA, Neumann G, Kawaoka Y.** 2012. Experimental adaptation of an influenza H5 HA confers respiratory droplet transmission to a reassortant H5 HA/H1N1 virus in ferrets. Nature **486:**420–428. http://dx.doi.org/10.1038/nature10831.
17. **Van Hoeven N, Pappas C, Belser JA, Maines TR, Zeng H, Garcia-Sastre**

A, Sasisekharan R, Katz JM, Tumpey TM. 2009. Human HA and polymerase subunit PB2 proteins confer transmission of an avian influenza virus through the air. Proc. Natl. Acad. Sci. U. S. A. **106:**3366–3371. http://dx.doi.org/10.1073/pnas.0813172106.

18. **Steel J, Lowen AC, Mubareka S, Palese P.** 2009. Transmission of influenza virus in a mammalian host is increased by PB2 amino acids 627K or 627E/701N. PLoS Pathog. **5:**e1000252. http://dx.doi.org/10.1371/journal.ppat.1000252.
19. **Maines TR, Chen LM, Matsuoka Y, Chen H, Rowe T, Ortin J, Falcon A, Nguyen TH, Mai Le Q, Sedyaningsih ER, Harun S, Tumpey TM, Donis RO, Cox NJ, Subbarao K, Katz JM.** 2006. Lack of transmission of H5N1 avian-human reassortant influenza viruses in a ferret model. Proc. Natl. Acad. Sci. U. S. A. **103:**12121–12126. http://dx.doi.org/10.1073/pnas.0605134103.
20. **Noton SL, Medcalf E, Fisher D, Mullin AE, Elton D, Digard P.** 2007. Identification of the domains of the influenza A virus M1 matrix protein required for NP binding, oligomerization and incorporation into virions. J. Gen. Virol. **88:**2280–2290. http://dx.doi.org/10.1099/vir.0.82809-0.
21. **Rossman JS, Lamb RA.** 2011. Influenza virus assembly and budding. Virology **411:**229–236. http://dx.doi.org/10.1016/j.virol.2010.12.003.
22. **Bui M, Whittaker G, Helenius A.** 1996. Effect of M1 protein and low pH on nuclear transport of influenza virus ribonucleoproteins. J. Virol. **70:**8391–8401.
23. **Rossman JS, Jing X, Leser GP, Lamb RA.** 2010. Influenza virus M2 protein mediates ESCRT-independent membrane scission. Cell **142:**902–913. http://dx.doi.org/10.1016/j.cell.2010.08.029.
24. **Ciampor F, Thompson CA, Grambas S, Hay AJ.** 1992. Regulation of pH by the M2 protein of influenza A viruses. Virus Res. **22:**247–258. http://dx.doi.org/10.1016/0168-1702(92)90056-F.
25. **Grambas S, Hay AJ.** 1992. Maturation of influenza A virus hemagglutinin–estimates of the pH encountered during transport and its regulation by the M2 protein. Virology **190:**11–18. http://dx.doi.org/10.1016/0042-6822(92)91187-Y.
26. **Shimbo K, Brassard DL, Lamb RA, Pinto LH.** 1996. Ion selectivity and activation of the M2 ion channel of influenza virus. Biophys. J. **70:**1335–1346. http://dx.doi.org/10.1016/S0006-3495(96)79690-X.
27. **Takeuchi K, Lamb RA.** 1994. Influenza virus M2 protein ion channel activity stabilizes the native form of fowl plague virus hemagglutinin during intracellular transport. J. Virol. **68:**911–919.
28. **Bourmakina SV, Garcia-Sastre A.** 2003. Reverse genetics studies on the filamentous morphology of influenza A virus. J. Gen. Virol. **84:**517–527. http://dx.doi.org/10.1099/vir.0.18803-0.
29. **Elleman CJ, Barclay WS.** 2004. The M1 matrix protein controls the filamentous phenotype of influenza A virus. Virology **321:**144–153. http://dx.doi.org/10.1016/j.virol.2003.12.009.
30. **Burleigh LM, Calder LJ, Skehel JJ, Steinhauer DA.** 2005. Influenza a viruses with mutations in the m1 helix six domain display a wide variety of morphological phenotypes. J. Virol. **79:**1262–1270. http://dx.doi.org/10.1128/JVI.79.2.1262-1270.2005.
31. **Bialas KM, Desmet EA, Takimoto T.** 2012. Specific residues in the 2009 H1N1 swine-origin influenza matrix protein influence virion morphology and efficiency of viral spread in vitro. PLoS One **7:**e50595. http://dx.doi.org/10.1371/journal.pone.0050595.
32. **Roberts PC, Lamb RA, Compans RW.** 1998. The M1 and M2 proteins of influenza A virus are important determinants in filamentous particle formation. Virology **240:**127–137. http://dx.doi.org/10.1006/viro.1997.8916.
33. **Rossman JS, Jing X, Leser GP, Balannik V, Pinto LH, Lamb RA.** 2010. Influenza virus m2 ion channel protein is necessary for filamentous virion formation. J. Virol. **84:**5078–5088. http://dx.doi.org/10.1128/JVI.00119-10.
34. **Seladi-Schulman J, Steel J, Lowen AC.** 2013. Spherical influenza viruses have a fitness advantage in embryonated eggs, while filament-producing strains are selected in vivo. J. Virol. **87:**13343–13353. http://dx.doi.org/10.1128/JVI.02004-13.
35. **Palese P, Shaw ML.** 2007. Orthomyxoviridae: the viruses and their replication, p 1648–1689. *In* Knipe DM, Howley PM, Griffin DE, Lamb RA, Martin MA, Roizman B, Straus SE (ed), Fields virology, 5th ed, vol 2. Lippincott Williams & Wilkins, Philadelphia, PA.
36. **Matrosovich MN, Matrosovich TY, Gray T, Roberts NA, Klenk HD.** 2004. Neuraminidase is important for the initiation of influenza virus infection in human airway epithelium. J. Virol. **78:**12665–12667. http://dx.doi.org/10.1128/JVI.78.22.12665-12667.2004.
37. **Wagner R, Matrosovich M, Klenk HD.** 2002. Functional balance between haemagglutinin and neuraminidase in influenza virus infections. Rev. Med. Virol. **12:**159–166. http://dx.doi.org/10.1002/rmv.352.
38. **Shtyrya Y, Mochalova L, Voznova G, Rudneva I, Shilov A, Kaverin N, Bovin N.** 2009. Adjustment of receptor-binding and neuraminidase substrate specificities in avian-human reassortant influenza viruses. Glycoconj. J. **26:**99–109. http://dx.doi.org/10.1007/s10719-008-9169-x.
39. **Lu B, Zhou H, Ye D, Kemble G, Jin H.** 2005. Improvement of influenza A/Fujian/411/02 (H3N2) virus growth in embryonated chicken eggs by balancing the hemagglutinin and neuraminidase activities, using reverse genetics. J. Virol. **79:**6763–6771. http://dx.doi.org/10.1128/JVI.79.11.6763-6771.2005.
40. **Das SR, Hensley SE, David A, Schmidt L, Gibbs JS, Puigbo P, Ince WL, Bennink JR, Yewdell JW.** 2011. Fitness costs limit influenza A virus hemagglutinin glycosylation as an immune evasion strategy. Proc. Natl. Acad. Sci. U. S. A. **108:**E1417–E1422. http://dx.doi.org/10.1073/pnas.1108754108.
41. **Das SR, Hensley SE, Ince WL, Brooke CB, Subba A, Delboy MG, Russ G, Gibbs JS, Bennink JR, Yewdell JW.** 2013. Defining influenza A virus hemagglutinin antigenic drift by sequential monoclonal antibody selection. Cell Host Microbe **13:**314–323. http://dx.doi.org/10.1016/j.chom.2013.02.008.
42. **Hensley SE, Das SR, Bailey AL, Schmidt LM, Hickman HD, Jayaraman A, Viswanathan K, Raman R, Sasisekharan R, Bennink JR, Yewdell JW.** 2009. Hemagglutinin receptor binding avidity drives influenza A virus antigenic drift. Science **326:**734–736. http://dx.doi.org/10.1126/science.1178258.
43. **Aoki FY, Boivin G, Roberts N.** 2007. Influenza virus susceptibility and resistance to oseltamivir. Antivir. Ther. **12:**603–616.
44. **Xu R, Zhu X, McBride R, Nycholat CM, Yu W, Paulson JC, Wilson IA.** 2012. Functional balance of the hemagglutinin and neuraminidase activities accompanies the emergence of the 2009 H1N1 influenza pandemic. J. Virol. **86:**9221–9232. http://dx.doi.org/10.1128/JVI.00697-12.
45. **National Research Council.** 2011. Guide for the care and use of laboratory animals. National Academies Press, Washington, DC.
46. **Lowen AC, Mubareka S, Tumpey TM, Garcia-Sastre A, Palese P.** 2006. The guinea pig as a transmission model for human influenza viruses. Proc. Natl. Acad. Sci. U. S. A. **103:**9988–9992. http://dx.doi.org/10.1073/pnas.0604157103.
47. **Fodor E, Devenish L, Engelhardt OG, Palese P, Brownlee GG, Garcia-Sastre A.** 1999. Rescue of influenza A virus from recombinant DNA. J. Virol. **73:**9679–9682.
48. **Chutinimitkul S, Herfst S, Steel J, Lowen AC, Ye J, van Riel D, Schrauwen EJ, Bestebroer TM, Koel B, Burke DF, Sutherland-Cash KH, Whittleston CS, Russell CA, Wales DJ, Smith DJ, Jonges M, Meijer A, Koopmans M, Rimmelzwaan GF, Kuiken T, Osterhaus AD, Garcia-Sastre A, Perez DR, Fouchier RA.** 2010. Virulence-associated substitution D222G in the hemagglutinin of 2009 pandemic influenza A(H1N1) virus affects receptor binding. J. Virol. **84:**11802–11813. http://dx.doi.org/10.1128/JVI.01136-10.
49. **Munster VJ, de Wit E, van den Brand JM, Herfst S, Schrauwen EJ, Bestebroer TM, van de Vijver D, Boucher CA, Koopmans M, Rimmelzwaan GF, Kuiken T, Osterhaus AD, Fouchier RA.** 2009. Pathogenesis and transmission of swine-origin 2009 A(H1N1) influenza virus in ferrets. Science **325:**481–483. http://dx.doi.org/10.1126/science.1177127.
50. **Gao Q, Brydon EW, Palese P.** 2008. A seven-segmented influenza A virus expressing the influenza C virus glycoprotein HEF. J. Virol. **82:**6419–6426. http://dx.doi.org/10.1128/JVI.00514-08.
51. **Steel J, Staeheli P, Mubareka S, Garcia-Sastre A, Palese P, Lowen AC.** 2010. Transmission of pandemic H1N1 influenza virus and impact of prior exposure to seasonal strains or interferon treatment. J. Virol. **84:**21–26. http://dx.doi.org/10.1128/JVI.01732-09.
52. **Steel J, Palese P, Lowen AC.** 2011. Transmission of a 2009 pandemic influenza virus shows a sensitivity to temperature and humidity similar to that of an H3N2 seasonal strain. J. Virol. **85:**1400–1402. http://dx.doi.org/10.1128/JVI.02186-10.
53. **Kaminski MM, Ohnemus A, Staeheli P, Rubbenstroth D.** 2013. Pandemic 2009 H1N1 influenza A virus carrying a Q136K mutation in the neuraminidase gene is resistant to zanamivir but exhibits reduced fitness in the guinea pig transmission model. J. Virol. **87:**1912–1915. http://dx.doi.org/10.1128/JVI.02507-12.
54. **Bouvier NM, Lowen AC, Palese P.** 2008. Oseltamivir-resistant influenza A viruses are transmitted efficiently among guinea pigs by direct contact

but not by aerosol. J. Virol. **82:**10052–10058. http://dx.doi.org/10.1128/JVI.01226-08.

55. **Shangguan T, Siegel DP, Lear JD, Axelsen PH, Alford D, Bentz J.** 1998. Morphological changes and fusogenic activity of influenza virus hemagglutinin. Biophys. J. **74:**54–62. http://dx.doi.org/10.1016/S0006-3495(98)77766-5.
56. **Itoh Y, Shinya K, Kiso M, Watanabe T, Sakoda Y, Hatta M, Muramoto Y, Tamura D, Sakai-Tagawa Y, Noda T, Sakabe S, Imai M, Hatta Y, Watanabe S, Li C, Yamada S, Fujii K, Murakami S, Imai H, Kakugawa S, Ito M, Takano R, Iwatsuki-Horimoto K, Shimojima M, Horimoto T, Goto H, Takahashi K, Makino A, Ishigaki H, Nakayama M, Okamatsu M, Warshauer D, Shult PA, Saito R, Suzuki H, Furuta Y, Yamashita M, Mitamura K, Nakano K, Nakamura M, Brockman-Schneider R, Mitamura H, Yamazaki M, Sugaya N, Suresh M, Ozawa M, Neumann G, Gern J, Kida H, Ogasawara K, Kawaoka Y.** 2009. In vitro and in vivo characterization of new swine-origin H1N1 influenza viruses. Nature **460:**1021–1025. http://dx.doi.org/10.1038/nature08260.
57. **Govorkova EA.** 2013. Consequences of resistance: in vitro fitness, in vivo infectivity, and transmissibility of oseltamivir-resistant influenza A viruses. Influenza Other Respir. Viruses **7**(Suppl. 1)**:**50–57. http://dx.doi.org/10.1111/irv.12044.
58. **Yen HL, Herlocher LM, Hoffmann E, Matrosovich MN, Monto AS, Webster RG, Govorkova EA.** 2005. Neuraminidase inhibitor-resistant influenza viruses may differ substantially in fitness and transmissibility. Antimicrob. Agents Chemother. **49:**4075–4084. http://dx.doi.org/10.1128/AAC.49.10.4075-4084.2005.
59. **Herlocher ML, Truscon R, Elias S, Yen HL, Roberts NA, Ohmit SE, Monto AS.** 2004. Influenza viruses resistant to the antiviral drug oseltamivir: transmission studies in ferrets. J. Infect. Dis. **190:**1627–1630. http://dx.doi.org/10.1086/424572.
60. **Bloom JD, Gong LI, Baltimore D.** 2010. Permissive secondary mutations enable the evolution of influenza oseltamivir resistance. Science **328:**1272–1275. http://dx.doi.org/10.1126/science.1187816.
61. **Ali A, Avalos RT, Ponimaskin E, Nayak DP.** 2000. Influenza virus assembly: effect of influenza virus glycoproteins on the membrane association of M1 protein. J. Virol. **74:**8709–8719. http://dx.doi.org/10.1128/JVI.74.18.8709-8719.2000.
62. **Barman S, Ali A, Hui EK, Adhikary L, Nayak DP.** 2001. Transport of viral proteins to the apical membranes and interaction of matrix protein with glycoproteins in the assembly of influenza viruses. Virus Res. **77:**61–69. http://dx.doi.org/10.1016/S0168-1702(01)00266-0.
63. **Mitnaul LJ, Castrucci MR, Murti KG, Kawaoka Y.** 1996. The cytoplasmic tail of influenza A virus neuraminidase (NA) affects NA incorporation into virions, virion morphology, and virulence in mice but is not essential for virus replication. J. Virol. **70:**873–879.